doi:10.1016/j.jmb.2008.07.045 J. Mol. Biol. (2008) 382, 638–651

JMB

Available online at www.sciencedirect.com

ScienceDirect

ELSEVIER

Hypertonia-Associated Protein Trak1 Is a Novel Regulator of Endosome-to-Lysosome Trafficking

Elizabeth Webber, Lian Li and Lih-Shen Chin*

Department of Pharmacology, Emory University School of Medicine, Atlanta, GA 30322-4218, USA

Received 21 April 2008; received in revised form 16 July 2008; accepted 17 July 2008
Available online
25 July 2008

Hypertonia, which is characterized by stiff gait, abnormal posture, jerky movements, and tremor, is associated with a number of neurological disorders, including cerebral palsy, dystonia, Parkinson's disease, stroke, and spinal cord injury. Recently, a spontaneous mutation in the gene encoding trafficking protein, kinesin-binding 1 (Trak1), was identified as the genetic defect that causes hypertonia in mice. The subcellular localization and biological function of Trak1 remain unclear. Here we report that Trak1 interacts with hepatocyte-growth-factor-regulated tyrosine kinase substrate (Hrs), an essential component of the endosomal sorting and trafficking machinery. Double-label immunofluorescence confocal studies show that the endogenous Trak1 protein partially colocalizes with Hrs on early endosomes. Like Hrs, both overexpression and small-interfering-RNA-mediated knockdown of Trak1 inhibit degradation of internalized epidermal growth factor receptors through a block in endosome-to-lysosome trafficking. Our findings support a role for Trak1 in the regulation of Hrs-mediated endosomal sorting and have important implications for understanding hypertonia associated with neurological disorders.

Edited by J. Karn

Keywords: endosome; Hrs; Trak1; trafficking; hypertonia

Introduction

Endosome-to-lysosome trafficking is a crucial step in the endocytic pathway that not only controls degradation of cell surface receptors but also regulates intracellular signaling.[1,2] Receptors at the cell surface are endocytosed either constitutively or in response to binding of their ligands and delivered to early endosomes. In the early endosomes, receptors are rapidly and specifically sorted between recycling and lysosomal degradation pathways. Lysosome-bound receptors, such as the epidermal growth factor receptor (EGFR), are recruited into invaginations of the early endosome's limiting membrane that then bud into the endosome lumen. The luminal contents of the endosome are delivered to the lysosome for degradation.[1,3] Recent studies have identified several components of the endosomal sorting machinery, including the hepatocyte-growth-factor-regulated tyrosine kinase substrate (Hrs) and the endosomal sorting complexes required for transport.[4–6] However, the molecular mechanisms that control endosomal sorting and trafficking are not fully understood.

The trafficking protein, kinesin-binding 1 (Trak1), also known as OIP106 [*O*-GlcNAc transferase (OGT)-*i*nteracting *p*rotein with a molecular mass of *106* kDa], is a 939-amino-acid protein initially identified as a binding partner for the enzyme β-*O*-linked *N*-acetylglucosamine (*O*-GlcNAc) transferase.[7,8] Subsequently, Trak1 has been shown to interact with kinesin heavy chain,[9] γ-amino-*n*-butyric acid A ($GABA_A$) receptor α1 subunit,[10] and mitochondrial Rho GTPases (Miro-1 and Miro-2).[11] However, the functional roles of these interactions have not yet been examined. Recently, a homozy-

*Corresponding author. E-mail address: chinl@pharm.emory.edu.

Abbreviations used: Trak1, trafficking protein, kinesin-binding 1; Hrs, hepatocyte-growth-factor-regulated tyrosine kinase substrate; EGFR, epidermal growth factor receptor; OGT, *O*-GlcNAc transferase; *O*-GlcNAc, β-O-linked *N*-acetylglucosamine; $GABA_A$, γ-amino-*n*-butyric acid A; HAP1, Huntingtin-associated protein 1; HAPN, HAP1 N-terminal domain; GRIF1, $GABA_A$-receptor-interacting factor 1; GFP, green fluorescent protein; HA, hemagglutinin A; KDEL, Lys-Asp-Glu-Leu; siRNA, small interfering RNA; WT, wild type; TIM23, translocase of inner membrane 23; EEA1, early endosome antigen 1; LAMP2, lysosomal-associated membrane protein 2; GST, glutathione *S*-transferase; TR, Texas Red; shRNA, small hairpin RNA; BSA, bovine serum albumin.

gous frameshift mutation in the mouse *Trak1* gene, which produces a protein truncated at amino acid 824, was found to cause a recessively transmitted form of hypertonia—a neurological dysfunction characterized by postural abnormalities, jerky movements, and tremor.[10] Hypertonia is observed in a variety of neurological disorders, including cerebral palsy, dystonia, Parkinson's disease, stroke, and spinal cord injury.[10] Despite genetic evidence indicating the importance of Trak1 in normal physiology, the cellular localization and biological function of Trak1 remain unclear.

In this study, we investigated the subcellular distribution and functional role of Trak1. Our results reveal that the endogenous Trak1 protein partially localizes to early endosomes, interacts with the endosomal sorting machinery component Hrs, and plays an essential role in the regulation of Hrs-mediated endosome-to-lysosome trafficking.

Results

Trak1 is a member of the Huntingtin-associated protein 1 N-terminal domain family

Mouse Trak1 is a 939-amino-acid protein that contains three putative coiled-coil domains (Fig. 1a).[12,13] The mouse hypertonia-associated Trak1 mutation[10] produces a mutant Trak1 protein truncated at residue 824 (Fig. 1a). Sequence analysis indicates that the mouse Trak1 protein shares a 92% overall amino acid identity with human Trak1 (Fig. 1b). The main difference between the 953-amino-acid human sequence and the 939-amino-acid mouse Trak1 sequence is an insertion of 12 residues (TVTSAIGG-LQLN) after residue 896 in the human Trak1 sequence. Aside from this insertion, the human and mouse Trak1 C-termini are virtually identical. As shown in Fig. 1b, Trak1 contains a Huntingtin-associated protein 1 (HAP1) N-terminal (HAPN) homologous domain, which encompasses the first two coiled-coil domains.[14] The HAPN domain is also found in two other mammalian proteins, HAP1 and $GABA_A$-receptor-interacting factor 1 (GRIF1), as well as in their *Drosophila* homologue, Milton (Fig. 1b).

In order to characterize the Trak1 protein, we generated a rabbit polyclonal anti-Trak1 antibody against residues 935–953 of human Trak1. To investigate the specificity of our anti-Trak1 antibody, immunoblot analysis was performed using cell lysates prepared from untransfected SH-SY5Y and HeLa cells, as well as transfected HeLa cells expressing green fluorescent protein (GFP)-tagged Trak1 (Fig. 1c). The anti-Trak1 antibody specifically recognized recombinant GFP-tagged Trak1 in transfected HeLa cell lysates, as well as the 115-kDa endogenous Trak1 protein in untransfected SH-SY5Y and HeLa cell lysates, consistent with a previous report.[7] In addition, the anti-Trak1 antibody also recognized a band at ~106 kDa (Fig. 1c, asterisk), which might represent a Trak1 degradation product because of its relative intensity as compared with the 115-kDa band varied from preparation to preparation. To further confirm the specificity of our anti-Trak1 antibody, we used two distinct small interfering RNA (siRNA) duplexes, Trak1 siRNA-1 and Trak1 siRNA-2, which specifically target different regions of the Trak1 mRNA, to deplete endogenous Trak1 protein in HeLa cells. Immunoblot analysis revealed that both Trak1-immunoreactive 115- and 106-kDa bands, but not the DJ1-immunoreactive band, disappeared upon treatment of cells with Trak1 siRNA-1 or Trak1 siRNA-2 (Fig. 1d). These results provide additional support for the specificity of our anti-Trak1 antibody and are consistent with the possibility that the 106-kDa band is a degradation product of Trak1.

The localization of Trak1 protein is poorly characterized and remains controversial. Iyer *et al.* reported that Trak1 immunoreactivity was present in the nucleus and in the cytoplasm of HeLa cells with a punctate pattern.[7] In contrast, Gilbert *et al.* found that Trak1 immunoreactivity was absent from nuclei and exhibited a diffuse cytosolic staining pattern in mouse brain tissue sections.[10] To determine whether our anti-Trak1 antibodies could be used for immunocytochemistry and to clarify the localization of Trak1, we performed immunofluorescence confocal microscopic analysis to determine the intracellular distribution of endogenous Trak1 and GFP-tagged Trak1 wild type (WT) in HeLa cells (Fig. 1e). We found an extensive overlap between the staining pattern detected by the anti-Trak1 antibody and the distribution pattern of GFP-tagged Trak1 WT visualized by the green fluorescence emitted by the GFP tag (Fig. 1e, upper panel), indicating that our anti-Trak1 antibody is able to recognize Trak1 protein by immunostaining. The endogenous Trak1 in untransfected HeLa cells, detected by the anti-Trak1 antibody, displays a punctate staining pattern that is excluded from the nucleus (Fig. 1e, upper panel, arrowhead), suggesting a vesicular localization for Trak1. In contrast, overexpression of Trak1 in transfected cells results in a tubular staining pattern (Fig. 1e, upper panel), consistent with previous reports.[9,11] This pattern is different from the punctate staining pattern of endogenous Trak1 (Fig. 1e, upper panel, arrowhead), suggesting that overexpression of Trak1 induces a change in Trak1 intracellular distribution.

To further confirm the specificity of our anti-Trak1 antibody in immunostaining, we transfected HeLa cells with Trak1 siRNA-2 or nontargeting control siRNA and then double-labeled the cells with anti-Trak1 antibody (to detect endogenous Trak1 protein) and with 4′,6-diamidino-2-phenylindole (to stain the nuclei). We observed the presence of Trak1-immunonegative cells only in Trak1 siRNA-transfected cultures (Fig. 1e, lower panel), but not in control siRNA-transfected cultures or in untransfected HeLa cell cultures (data not shown), suggesting that Trak1 siRNA treatment resulted in the loss of Trak1 immunoreactivity. These data, together with the result of immunostaining in GFP-Trak1-transfected cells (Fig. 1e, upper panel) and the results of our antibody characterization by Western blot analysis

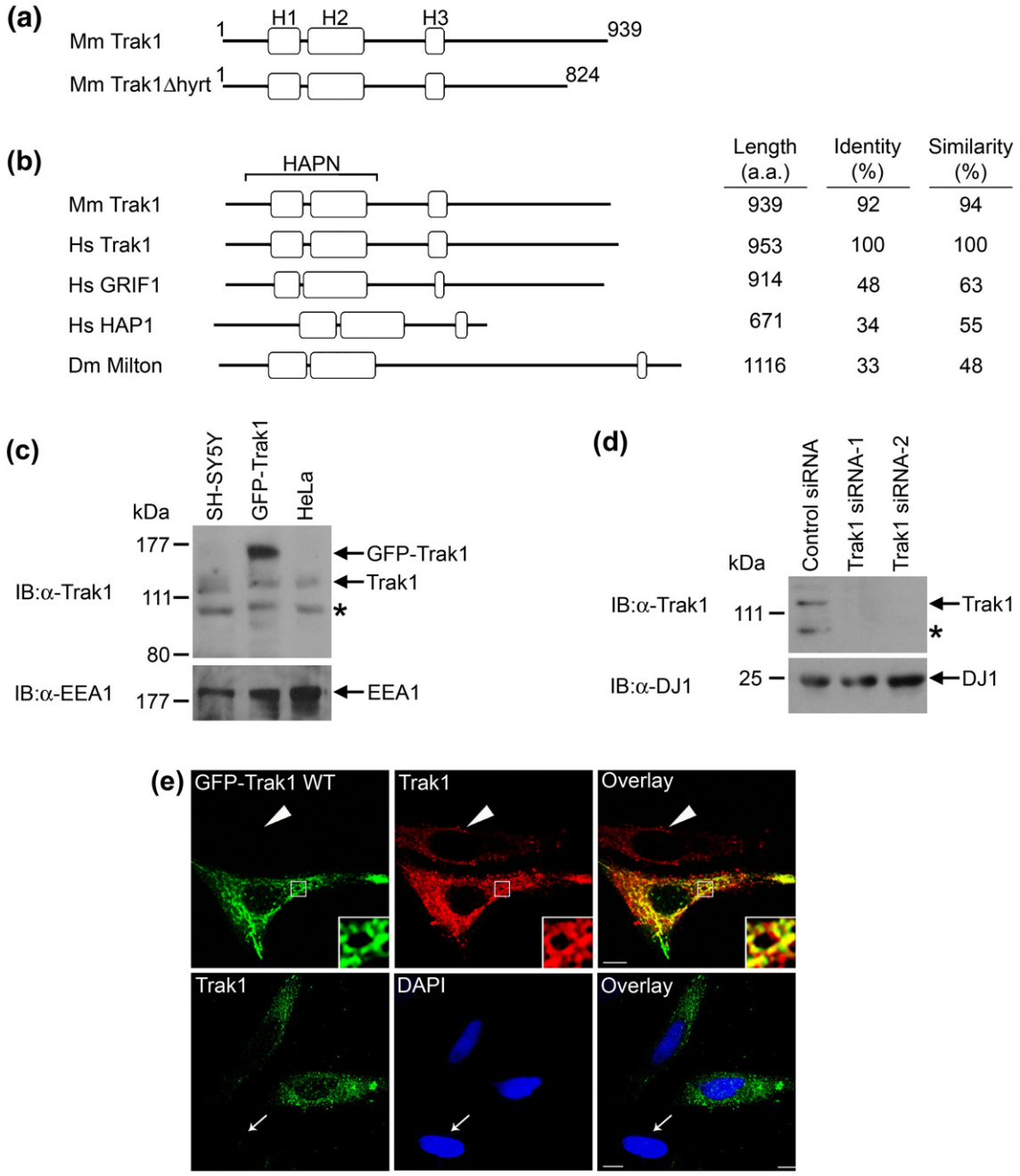

Fig. 1. Characterization of anti-Trak1 antibodies. (a) Domain structure of full-length mouse Trak1 (top) and the truncated Trak1 produced in *hyrt* mutant mice (bottom). White boxes indicate the location of the predicted coiled-coil regions for mouse Trak1. (b) Domain structure of Trak1 and its homologues. Accession numbers are as follows: *Mm* Trak1, NP_780323; *Hs* Trak1, NP_001036111; *Hs* GRIF1, NP_055864; *Hs* HAP1, NP_003940; and *Dm* Milton, NP_723249. The amino acid identity and similarity of each protein relative to the protein sequence of human Trak1 are indicated. Each protein contains three predicted coiled-coil domains shown as white boxes. *Mm* Trak1: 103–185, 207–356, and 489–529; *Hs* Trak1: 104–186, 207–356, and 492–532; *Hs* GRIF1: 126–170, 198–354, and 507–519; *Hs* HAP1: 212–293, 307–427, 431–460, and 593–606; *Dm* Milton: 133–209, 226–377, and 1021–1034. The bracket indicates the location of the HAPN domain. *Mm* Trak1: 46–353; *Hs* Trak1: 47–354; *Hs* GRIF1: 47–354; *Hs* HAP1: 106–460; *Dm* Milton: 75–376. *Mm*, *Mus musculus*; *Hs*, *Homo sapiens*; *Dm*, *Drosophila melanogaster*. (c) Specificity of the anti-Trak1 antibody. Western blot analysis of cell lysates from SH-SY5Y, HeLa, and pGFP-Trak1-transfected HeLa cells using anti-Trak1 and anti-EEA1 antibodies. The asterisk indicates a band that appears specific for the anti-Trak1 antibody. (d) HeLa cells were transiently transfected with 100 nM of the indicated siRNA constructs. Whole-cell lysates were subjected to SDS-PAGE, followed by immunoblotting with anti-Trak1 antibody. Equal loading was confirmed by immunoblotting with anti-DJ1 antibody. The asterisk indicates a band that appears specific to the anti-Trak1 antibody. (e) Upper panel: HeLa cells were transfected with GFP-Trak1 WT (green) and then immunostained using anti-Trak1 antibody (red). Arrowhead indicates an untransfected cell. Lower panel: HeLa cells were transfected with Trak1 siRNA-2 and then immunostained using anti-Trak1 antibody (green). Nuclei were stained using 4′,6-diamidino-2-phenylindole. Arrow indicates a transfected cell. The scale bar represents 10 μm.

(Fig. 1c and d), provide strong evidence supporting the specificity of our anti-Trak1 antibody.

A population of endogenous Trak1 is localized to early endosomes

To further characterize the subcellular distribution of Trak1, we compared the distribution of endogenous Trak1 with that of various organelle marker proteins using double-label immunofluorescence confocal microscopy (Fig. 2). Previous studies reported the presence of epitope-tagged Trak1 in mitochondria;[9,11] however, it is unclear whether the endogenous Trak1 protein also localizes to mitochondria. To test this possibility, we first compared endogenous Trak1 staining with that of the mitochondrial marker translocase of inner membrane 23 (TIM23). We observed a partial overlap (39.4±3.0%) between Trak1 and TIM23 immunoreactivities (Fig. 2) indicating that a subset of Trak1 localizes to mitochondria. The lack of complete overlap suggested that Trak1 is not restricted to the mitochondrial compartment. Given the reported localization of other HAPN proteins to early endosomes,[14,15] we next compared Trak1 staining with that of the early endosomal markers Hrs and early endosome antigen 1 (EEA1). Endogenous Trak1 overlaps by 64.3±3.7% with Hrs and by 45.1±4.8% with EEA1 (Fig. 2), indicating that a population of Trak1 is associated with early endosomes. In contrast, we observed a 21.8±2.1% overlap between Trak1 and the late endosome/lysosome marker lysosomal-associated membrane protein 2 (LAMP2), and 21.2±3.0% of Trak1 overlapped with the endoplasmic reticulum marker Lys-Asp-Glu-Leu (KDEL) (Fig. 2). Together, these findings indicate that Trak1 is associated with both mitochondria and endosomes; however, our data suggest that Trak1 is predominantly associated with early endosomes (Fig. 2b).

Trak1 interacts with Hrs *in vivo* and *in vitro*

Trak1 is a member of the HAPN family, which also includes the Hrs-binding proteins HAP1 and GRIF1.[14,15] The Hrs-binding region of rat GRIF1 (residues 359–507)[14] shows a 50% amino acid similarity to the corresponding region (residues 359–507) of human Trak1. This observation, along with our data showing that Trak1 localizes to early endosomes (Fig. 2), raises the possibility that Trak1 may associate with Hrs. To examine this possibility, we first performed coimmunoprecipitation experiments using lysates from HeLa cells cotransfected with pGFP-Trak1 and pHA-Hrs or pHA vector (Fig. 3a). Immunoprecipitation of the lysates with an anti-hemagglutinin A (HA) antibody revealed that GFP-Trak1 was specifically coimmunoprecipitated with HA-Hrs, but not with the HA vector control. We then performed additional coimmunoprecipitation experiments to examine the association of endogenous Trak1 and Hrs in HeLa cells (Fig. 3b). The anti-Trak1 antibody, but not the preimmune serum, was able to coimmunoprecipitate Trak1 and Hrs from

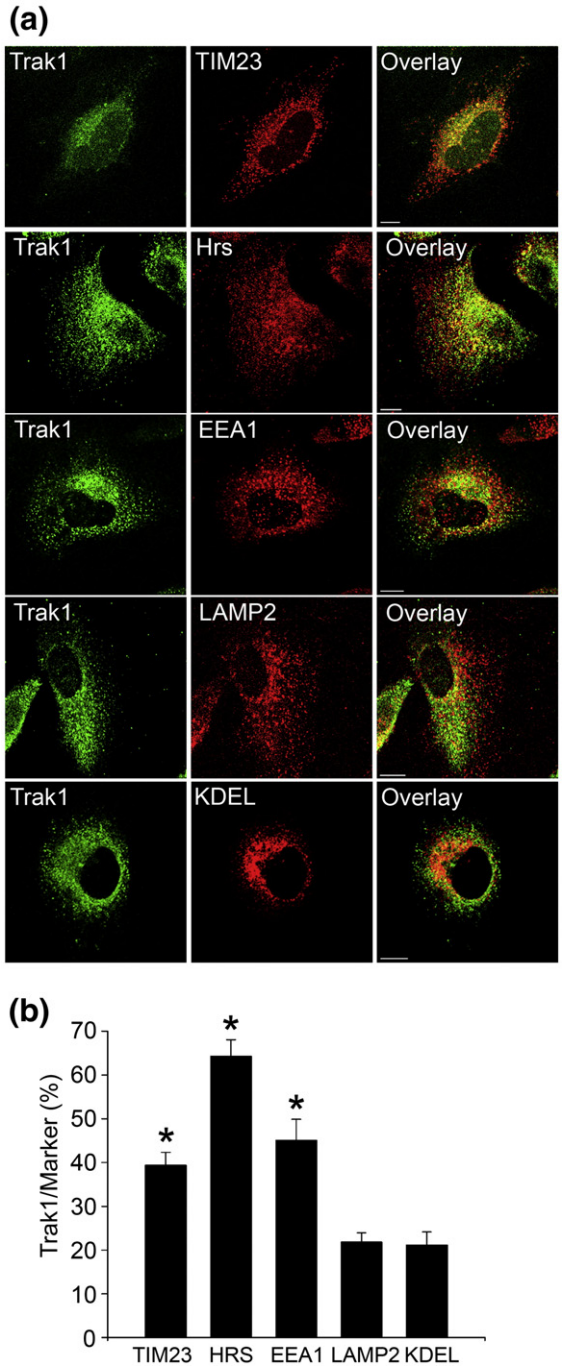

Fig. 2. Endogenous localization of Trak1. (a) HeLa cells were double-immunostained using anti-Trak1 antibody and anti-TIM23, anti-Hrs, anti-EEA1, anti-LAMP2, and anti-KDEL antibodies. The scale bar represents 10 μm. (b) Quantification of Trak1 localization in HeLa cells. Images were processed and analyzed as described in Materials and Methods. The percentage of Trak1 that overlaps with the indicated marker proteins is presented as mean±SEM. The asterisks indicate a statistically significant difference ($p<0.05$) from the KDEL results. Data are the result of three to five separate experiments.

HeLa cell lysates, demonstrating the existence of an endogenous Hrs–Trak1 complex (Fig. 3b). To verify that the interaction between Hrs and Trak1 is direct,

we performed *in vitro* binding assays using recombinant Hrs and Trak1 proteins. Glutathione *S*-transferase (GST) or GST–Trak1 fusion proteins immobilized on glutathione agarose beads were incubated with soluble His-tagged Hrs. As shown in Fig. 3c, His-Hrs is specifically bound by GST–Trak1 and not by the GST control, indicating a direct and specific interaction between recombinant Hrs and Trak1.

To further define the interaction between Trak1 and Hrs, we generated two GST-tagged Trak1 deletion constructs (Fig. 4a): Trak1Δ1, which encodes the N-terminal region, and Trak1Δ2, which encodes the C-terminal region that includes the predicted Hrs-binding domain (residues 359–507). Only the GST fusion proteins containing the predicted Hrs-binding region (Trak1 and Trak1Δ2) were capable of binding Hrs (Fig. 4b). The GST–Trak1Δ1 fusion protein did not interact with Hrs, suggesting that the conserved Hrs-binding region in Trak1, which was first

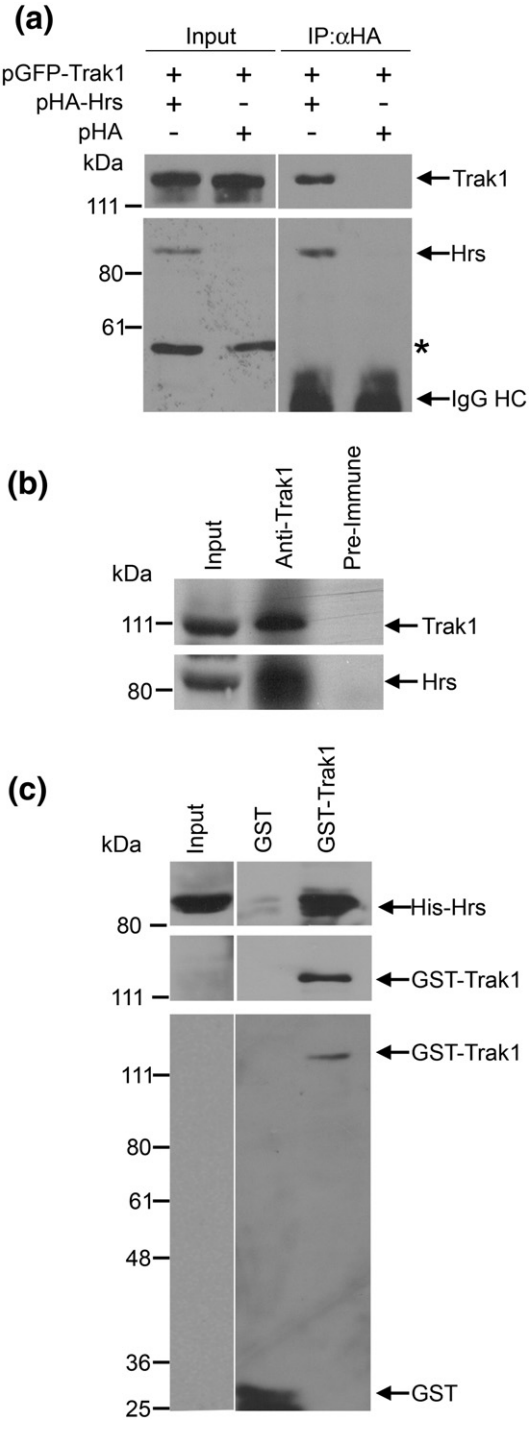

Fig. 3. Trak1 and Hrs associate *in vivo* and *in vitro*. (a) Coimmunoprecipitation of Trak1 with Hrs in transfected HeLa cells. HeLa cells were cotransfected with pGFP-Trak1 in combination with pHA-Hrs or pHA vector. Lysates were immunoprecipitated with anti-HA antibody, followed by immunoblotting with anti-GFP and anti-HA antibodies. The asterisk indicates a nonspecific band. (b) Coimmunoprecipitation of endogenous Hrs with Trak1 in HeLa cells. HeLa cell lysates were immunoprecipitated with anti-Trak1 antibody or preimmune serum, followed by immunoblotting for Hrs and Trak1. (c) *In vitro* association between Hrs and Trak1. Soluble His-tagged Hrs was incubated with equal amounts of immobilized GST or GST–Trak1 fusion proteins. Bound His-Hrs and immobilized GST fusion proteins were detected by immunoblotting with anti-Hrs, anti-Trak1, and anti-GST antibodies.

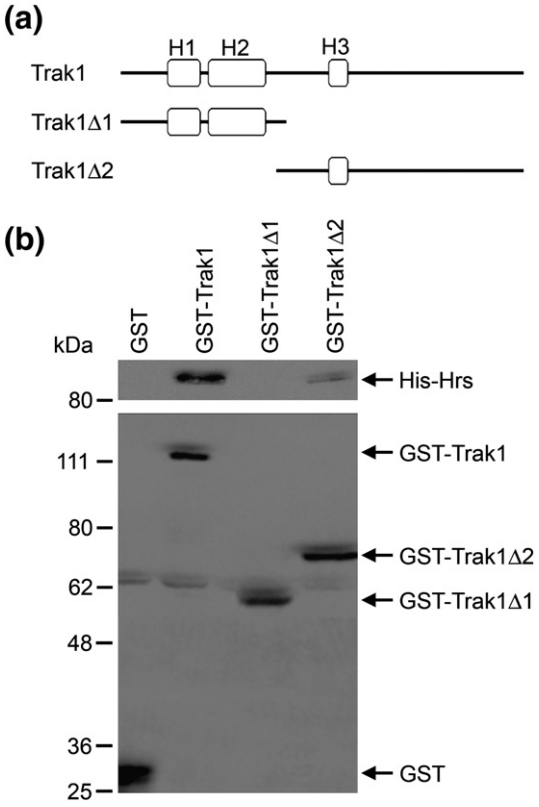

Fig. 4. Mapping the Hrs-binding region of Trak1. (a) Domain structure of Trak1 and its deletion mutants encoded by GST-tagged cDNA constructs. (b) Soluble His-tagged Hrs was incubated with equal amounts of immobilized GST or GST fusion proteins. Bound His-Hrs and immobilized GST fusion proteins were detected by immunoblotting with anti-Hrs and anti-GST antibodies, respectively.

identified in GRIF1,[14] is required for the interaction between Hrs and Trak1.

Localization of Trak1 to early endosomes is dependent on the presence of the Hrs-binding domain

As a first step towards investigating the pathogenic effects of hypertonia-associated Trak1 mutation, we generated a truncated Trak1Δhyrt (residues 1–824) construct to assess whether the Trak1 truncation mutation found in *hyrt* mice[10] would impact the subcellular localization of Trak1 (Fig. 5a). Using double-label immunofluorescence microscopy, we compared the distribution of the Trak1 WT and Trak1Δhyrt mutant with Hrs (Fig. 5b). An overlap of 51.1 ± 4.5% between GFP-tagged Trak1 WT and Hrs staining was observed (Fig. 5b and c). The GFP-tagged Trak1Δhyrt mutant showed a 53.3±2.1% overlap with Hrs, which appears to be indistinguishable from that of GFP-Trak1 WT (Fig. 5b and c), suggesting that the *hyrt* mutation does not affect the localization of Trak1 to Hrs-positive early endosomes.

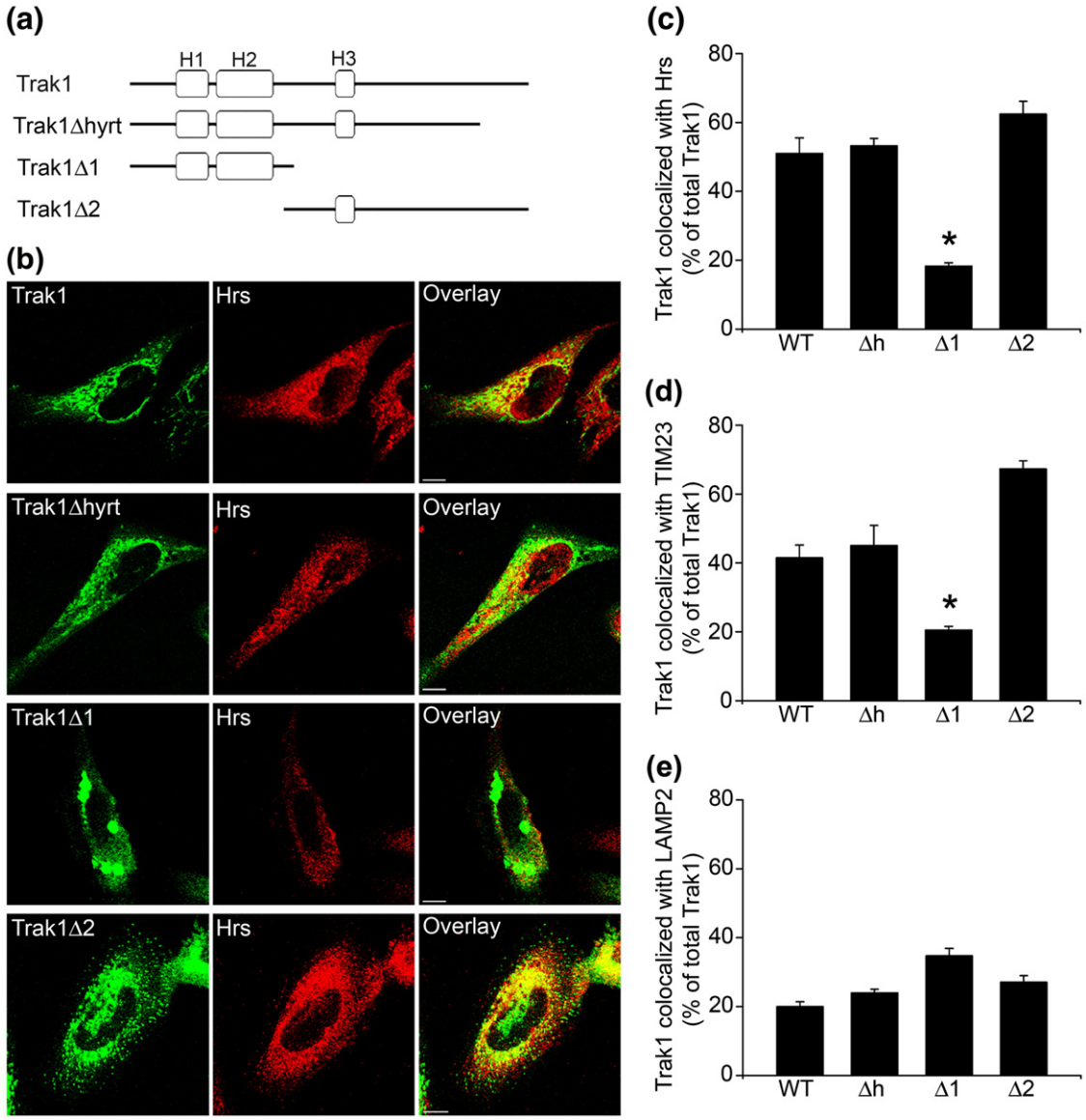

Fig. 5. The C-terminal region of Trak1 is required for the early endosomal and mitochondrial localization of Trak1. (a) Domain structure of Trak1 and its deletion mutants encoded by GFP-tagged cDNA constructs. (b) HeLa cells were transiently transfected with pGFP-Trak1, pGFP-Trak1Δhyrt, pGFP-Trak1Δ1, or pGFP-Trak1Δ2. GFP-Trak1 was visualized by the green fluorescence emitted by the GFP tag, and endogenous Hrs was detected using an anti-Hrs antibody (red). The scale bar represents 10 μm. (c–e) HeLa cells were transiently transfected with pGFP-Trak1 (WT), pGFP-Trak1Δhyrt (Δh), pGFP-Trak1Δ1 (Δ1), or pGFP-Trak1Δ2 (Δ2). GFP-Trak1 was visualized by the green fluorescence emitted by the GFP tag, and cells were immunostained using anti-Hrs (c), anti-TIM23 (d), and anti-LAMP2 (e) antibodies. Images were processed and analyzed as described in Materials and Methods. The percentage of Trak1 that overlaps with the indicated marker proteins is presented as mean±SEM. The asterisks indicate a statistically significant difference ($p<0.05$) from the WT results. Data are the result of three to five separate experiments.

Next, we used the N-terminal region construct (Trak1Δ1) and the C-terminal region construct (Trak1Δ2) to test the effect of the Hrs-binding region on Trak1 localization (Fig. 5a). The C-terminal GFP-Trak1Δ2 mutant did not exhibit the WT staining pattern; however, an overlap of 62.5 ± 3.7% between GFP-Trak1Δ2 and Hrs was still observed (Fig. 5b and c). In contrast, GFP-tagged Trak1Δ1 only displayed an 18.3 ± 0.9% overlap with Hrs staining (Fig. 5b and c). These findings suggest that the presence of the Hrs-binding domain is necessary in targeting Trak1 to Hrs-positive early endosomes.

To further characterize the intracellular distribution of the Trak1 deletion mutants, we quantified the overlap between our GFP-tagged Trak1 proteins and TIM23 (Fig. 5d) and LAMP2 (Fig. 5e). Full-length GFP-tagged Trak1, Trak1Δhyrt, and Trak1Δ2 overlap by 41.5±3.7%, 45.1±5.8%, and 67.4±2.3% with TIM23, respectively (Fig. 5d). GFP-tagged Trak1Δ1 only showed a 20.1±1.0% overlap with TIM23 (Fig. 5d). Endogenous Trak1 labeling was not observed to significantly overlap with LAMP2 (Fig. 2b); in agreement with this, we did not observe any statistically significant changes in the overlap observed between full-length GFP-tagged Trak1, Trak1Δhyrt, Trak1Δ1, and Trak1Δ2 (Fig. 5e). However, we did observe a trend, which failed to reach statistical significance, of colocalization between Trak1Δ1 and LAMP2, suggesting an increased localization to late endosomes/lysosomes. Overexpressed Trak1Δ1 forms inclusions (Fig. 5b) that may be processed through autophagy,[16,17] hence the increased localization of Trak1Δ1 to lysosomes (Fig. 5e). These results suggest that, although the deletion of the N-terminal region in Trak1Δ2 produces a staining pattern that is distinct from that of full-length Trak1 (Fig. 5b), it is similarly distributed to early endosomes and mitochondria (Fig. 5c and d). Furthermore, the ability of Trak1Δ2, but not Trak1Δ1, to localize to early endosomes and mitochondria supports the idea that the C-terminal region of Trak1 contains the conserved Hrs-binding[14] and Miro-binding[18] domains.

Overexpression of Trak1 and its mutants inhibits EGF-induced EGFR degradation, but not endocytosis

EGF-induced degradation of the EGFR is a widely used model for studying endocytic trafficking. Binding of EGF to the EGFR at the cell surface triggers rapid internalization of the EGF–EGFR complex and subsequent sorting at the early endosomes for lysosomal degradation.[19–21] The role of Hrs in regulating endosomal trafficking of EGFR has been well established; both overexpression and knockdown of Hrs inhibit ligand-induced EGFR degradation.[22,23] The observed interaction and colocalization of Trak1 with Hrs thus raise the possibility that Trak1 may participate in the regulation of EGF-induced endocytic trafficking of EGFR to the lysosome for degradation. To test this possibility, we assessed the effects of overexpressing WT and mutant Trak1 on EGF-induced EGFR internalization

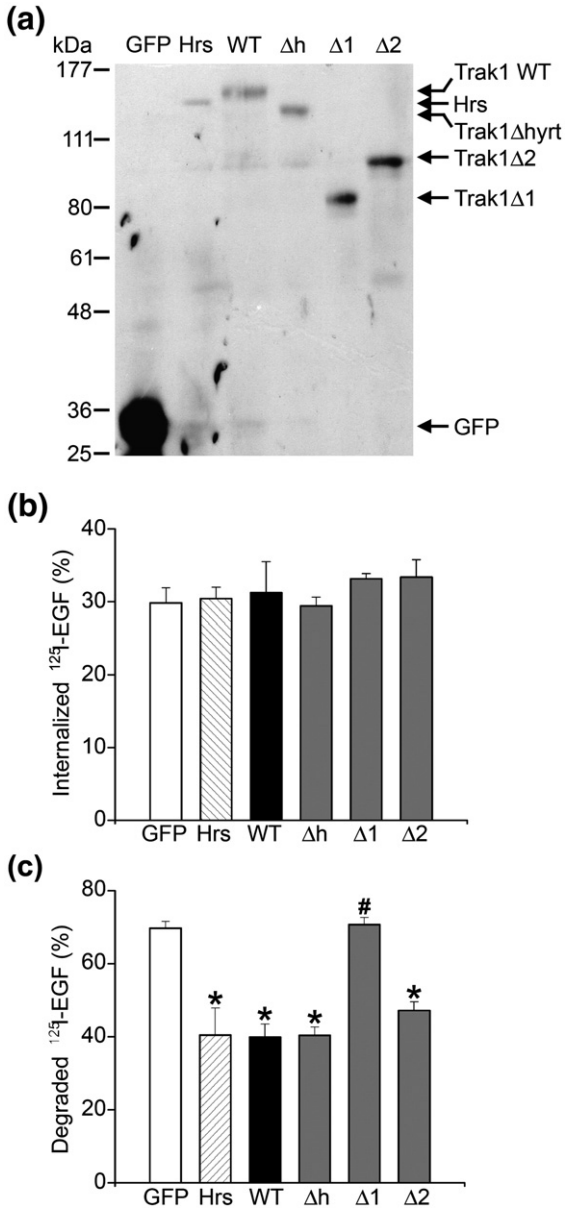

Fig. 6. Trak1 inhibits the degradation of EGF–EGFR complexes, and this action depends on the interaction with Hrs. (a) Lysates from HeLa cells transfected with the indicated GFP-tagged expression constructs were subjected to SDS-PAGE, followed by immunoblotting with anti-GFP antibody. (b) Trak1 overexpression has no effect on [^{125}I]EGF uptake. HeLa cells were transiently transfected with GFP vector, GFP-tagged Hrs (Hrs), or the following GFP-tagged Trak1 constructs: Trak1 (WT), Trak1Δhyrt (Δh), Trak1Δ1 (Δ1), or Trak1Δ2 (Δ2). Cells were incubated with [^{125}I]EGF for 10 min at 37 °C. The internalized [^{125}I]EGF is expressed as a percentage of the initially bound [^{125}I]EGF. (c) HeLa cells transfected with the indicated constructs were allowed to internalize [^{125}I]EGF for 10 min and then chased for 1 h at 37 °C. The degraded [^{125}I]EGF is expressed as a percentage of the initially internalized [^{125}I]EGF. Data represent the mean± SEM from three independent experiments. The asterisks indicate a statistically significant difference ($p<0.05$) from the vector-transfected cells, whereas the pound sign indicates a statistically significant difference ($p<0.05$) from the GFP-Trak1 WT-transfected cells.

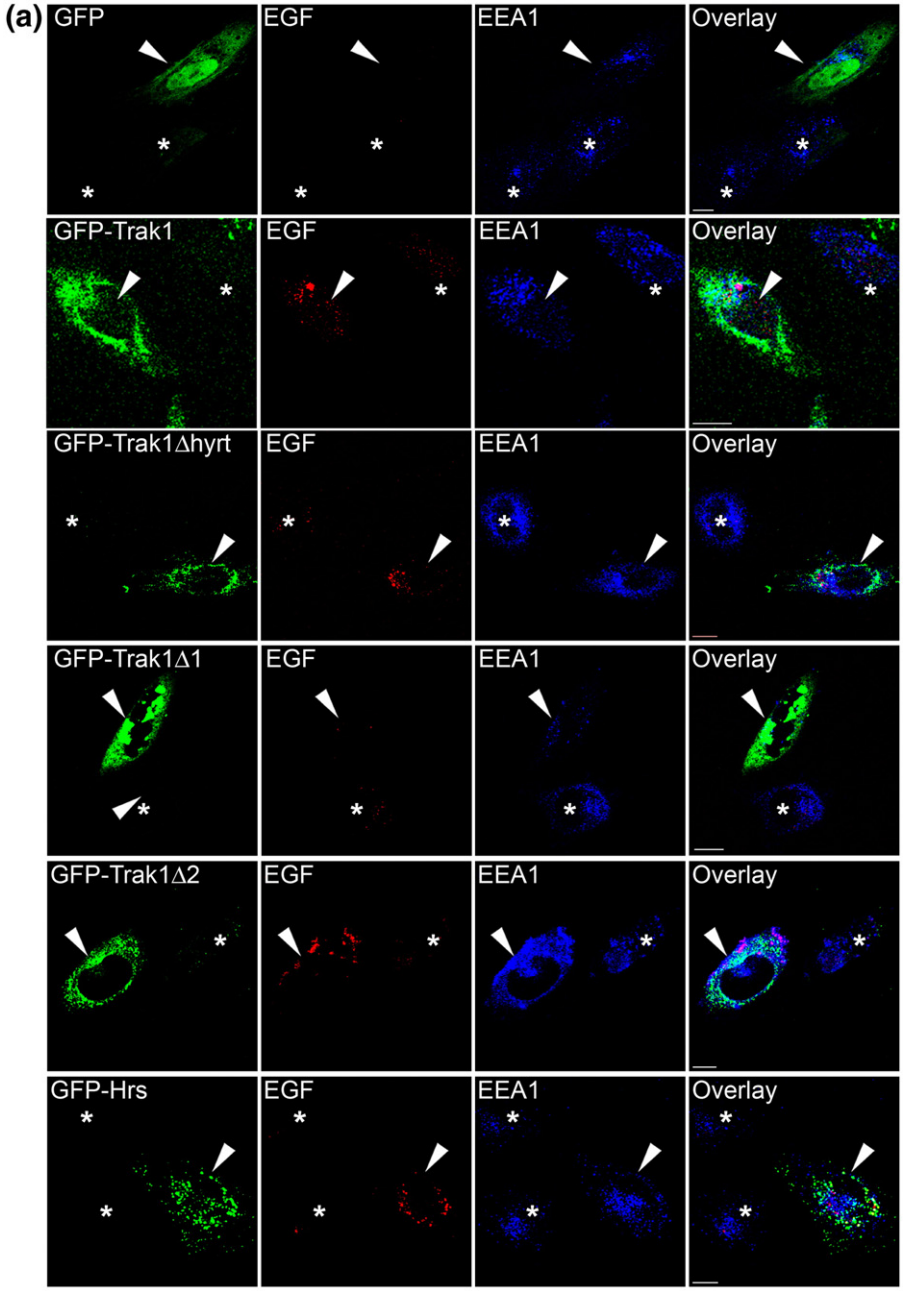

Fig. 7 *(legend on next page)*

and degradation, using the overexpression of Hrs as positive control. HeLa cells were transfected with the indicated GFP-tagged Trak1 WT and deletion constructs, or GFP-Hrs, and the expression of these proteins was confirmed by Western blot analysis (Fig. 6a). Biochemical analysis of endocytosis using a quantitative [^{125}I]EGF uptake assay showed that cells overexpressing WT or mutant Trak1 internalized an amount of [^{125}I]EGF similar to those of the GFP-transfected or GFP-Hrs-transfected controls (Fig. 6b). In addition, cell-based assays of endocytosis with Texas Red (TR)-conjugated EGF or TR-transferrin also showed that cells overexpressing WT or mutant Trak1 internalized amounts of TR-EGF and TR-transferrin similar to those of the GFP-transfected or GFP-Hrs-transfected controls (data not shown). Together, these results indicate that, like Hrs,[22,23] overexpression of WT or mutant Trak1 had no significant effect on constitutive or regulated endocytosis.

We next examined and compared the effects of overexpressing WT or mutant Trak1 and Hrs on EGF-induced EGFR degradation using a quantitative [^{125}I]EGF degradation assay. In this assay, cells were allowed to internalize [^{125}I]EGF for 10 min. After the cells had been washed to remove extracellular and surface-bound [^{125}I]EGF, they were chased at 37 °C for 1, 2, or 3 h to allow degradation. As shown in Fig. 6c, in the GFP-transfected control cells, 69.7±1.9% ($n=3$) of internalized [^{125}I]EGF was degraded after the 1-h chase. Overexpression of full-length Trak1 significantly decreased the degradation of [^{125}I]EGF to 39.9±3.6% ($n=3$; $p<0.001$), which is similar to the effect exerted by overexpression of Hrs (40.5±7.4%; $n=3$; $p<0.001$). A similar extent of reduction in [^{125}I]EGF degradation was also observed in cells overexpressing Trak1 deletion mutants that contain the Hrs-binding domain, specifically Trak1Δhyrt (40.3±2.2%; $n=3$; $p<0.001$) and Trak1Δ2 (47.1±2.4%; $n=3$; $p<0.001$). In contrast, the amount of degraded [^{125}I]EGF in cells overexpressing Trak1Δ1 (70.8±1.9%; $n=3$) was not significantly different from that in the GFP-transfected control cells. Similar effects of overexpressing WT and mutant Trak1 on [^{125}I]EGF degradation were also seen at the 2- and 3-h chase time points (data not shown). These data, together with the result obtained from an analysis of the effects of Trak1 deletions on colocalization with Hrs (Fig. 5), suggest that the association of Trak1 with Hrs-positive early endosomes is required for the inhibitory effect of Trak1 overexpression on EGF-induced EGFR degradation.

Trak1 regulates endosome-to-lysosome trafficking of internalized EGFR

To assess the effect of Trak1 overexpression on endosome-to-lysosome trafficking of EGF–EGFR complexes, we used a "pulse-chase" trafficking assay.[14,15] In this assay, HeLa cells were allowed to internalize TR-EGF for 10 min, and the fate of internalized TR-EGF after a 1-, 2-, or 3-h chase period was monitored by fluorescence confocal microscopy (Fig. 7a). We found that the TR-EGF fluorescence signal in untransfected cells was dramatically reduced after the 1-h chase, indicating that most of the internalized TR-EGF had been degraded (Fig. 7a, asterisks). In comparison, cells overexpressing Trak1 retained a significant amount of the internalized TR-EGF after the same 1-h chase period (Fig. 7a, arrowheads), suggesting that the trafficking from the early endosome to the lysosome is impeded by Trak1 overexpression. Quantification analysis (Fig. 7b) revealed that, in untransfected cells, 10.9±1.2% of the internalized TR-EGF remained after the 1-h chase, which is similar to the amount of remaining TR-EGF (10.5±0.8%) found in GFP-transfected cells. The amount of remaining TR-EGF was significantly increased ($p<0.001$) in Trak1-overexpressing cells (27.0±3.3%), as well as in Hrs-overexpressing cells (25.9±5.3%), suggesting that Trak1 overexpression inhibits endosome-to-lysosome trafficking to a similar extent as Hrs overexpression. Moreover, we found that the amount of remaining TR-EGF was increased in cells expressing Trak1Δhyrt (24.8±6.9%) and Trak1Δ2 (30.2±1.5%), but not in cells expressing Trak1Δ1 (10.5±0.5%), indicating that only the Trak1 deletion mutants containing the conserved Hrs-binding region are capable of inhibiting trafficking, whereas the Trak1 deletion mutant lacking the Hrs-binding region had no effect. Similar effects of overexpressing WT and mutant Trak1 on the degradative trafficking of internalized TR-EGF were also seen at the 2- and 3-h chase time points (data not shown). These data obtained from the TR-EGF trafficking assays are in agreement with the results of our [^{125}I]EGF degradation assays (Fig. 6c) and suggest that Trak1 regulates EGF-induced EGFR trafficking from the early endosome to the lysosome in an Hrs-dependent manner.

Fig. 7. Trak1 overexpression inhibits trafficking of EGF–EGFR complexes from early endosomes to the lysosomal pathway. (a) HeLa cells expressing GFP or GFP-tagged Trak1, Trak1Δhyrt, Trak1Δ1, Trak1Δ2, and Hrs were allowed to internalize TR-EGF for 10 min and then chased for 1 h at 37 °C. Cells were stained with a primary antibody against EEA1 and a CY5-conjugated secondary antibody. Arrowheads and asterisks indicate transfected and untransfected cells, respectively. The scale bar represents 10 μm. (b) HeLa cells were transiently transfected with the GFP vector, GFP-tagged Hrs (Hrs), or the following GFP-tagged Trak1 constructs: Trak1 (WT), Trak1Δhyrt (Δh), Trak1Δ1 (Δ1), or Trak1Δ2 (Δ2). Untransfected HeLa cells were used as control (CTL). The amount of remaining TR-EGF after a 1-h chase was quantified and expressed as a percentage of the initially internalized TR-EGF. Data represent the mean±SEM from three independent experiments. The asterisks indicate a statistically significant difference ($p<0.05$) from the GFP-vector-transfected cells, whereas the pound sign indicates a statistically significant difference ($p<0.05$) from the GFP-Trak1 WT-transfected cells.

Trak1 is essential for ligand-induced EGFR degradation

To provide further evidence supporting the role of Trak1 in the regulation of EGFR trafficking, we examined the effect of siRNA-mediated knockdown of Trak1 expression on the uptake and degradation of [^{125}I]EGF in HeLa cells, using the knockdown of Hrs as positive control. For selective depletion of endogenous Trak1 or Hrs, HeLa cells were transfected with Trak1 siRNA-1, Trak1 siRNA-2, Hrs siRNA-1, or Hrs siRNA-2. Immunoblot analysis of transfected cell lysates confirmed the knockdown of endogenous Trak1 or Hrs (Fig. 8a). We found that depletion of Trak1 or Hrs had no statistically significant effect on [^{125}I]EGF internalization (Fig. 8b). As shown in Fig. 8c, we observed a statistically significant ($p<0.001$) decrease in [^{125}I]EGF degradation in both Trak1 siRNA-1-transfected (36.2±5.2%; $n=3$) and Trak1 siRNA-2-transfected (32.1±7.1%; $n=3$) HeLa cells compared to the control siRNA-transfected cells (64.1±2.8%; $n=3$) after the 1-h chase. The effect of Trak1 depletion on [^{125}I]EGF degradation is comparable to the effect exerted by Hrs depletion from treatment with Hrs siRNA-1 (31.9±9.2%; $n=3$) and Hrs siRNA-2 (35.5±10.5%; $n=3$). Similar effects of Trak1 and Hrs on [^{125}I]EGF degradation were also seen at the 2- and 3-h chase time points (data not shown). Together, these data provide strong evidence supporting a functional role for Trak1 in regulating the trafficking of internalized EGF–EGFR complexes to the lysosome for degradation.

Discussion

Recent identification of a homozygous frameshift mutation in mouse Trak1 as the cause of a recessively transmitted form of hypertonia[10] highlights the importance of understanding the cellular role of Trak1, a newly discovered protein of unknown function. In the current study, we found that Trak1 interacts with the endosomal sorting machinery component Hrs and provided evidence supporting a role for Trak1 as a novel regulator of endosome-to-lysosome trafficking.

The subcellular localization of Trak1 is poorly defined; previous studies reported localization of Trak1 in the nucleus,[7] cytosol,[10] mitochondria,[9,11] and vesicular structures of unknown identity.[7] To clarify the subcellular localization of Trak1, we generated a specific anti-Trak1 antibody and found that endogenous Trak1 is partially localized to mitochondria, in agreement with the reported interaction of Trak1 with the mitochondrial Miro proteins.[11] Interestingly, our studies revealed that a population of endogenous Trak1 is associated with Hrs- and EEA1-positive early endosomes. Furthermore, deletion analysis showed that the localization of Trak1 to early endosomes depends on its interaction with Hrs. These data suggest that Trak1 is appropriately localized to influence Hrs-mediated endosomal sorting. In support of this view, our functional studies

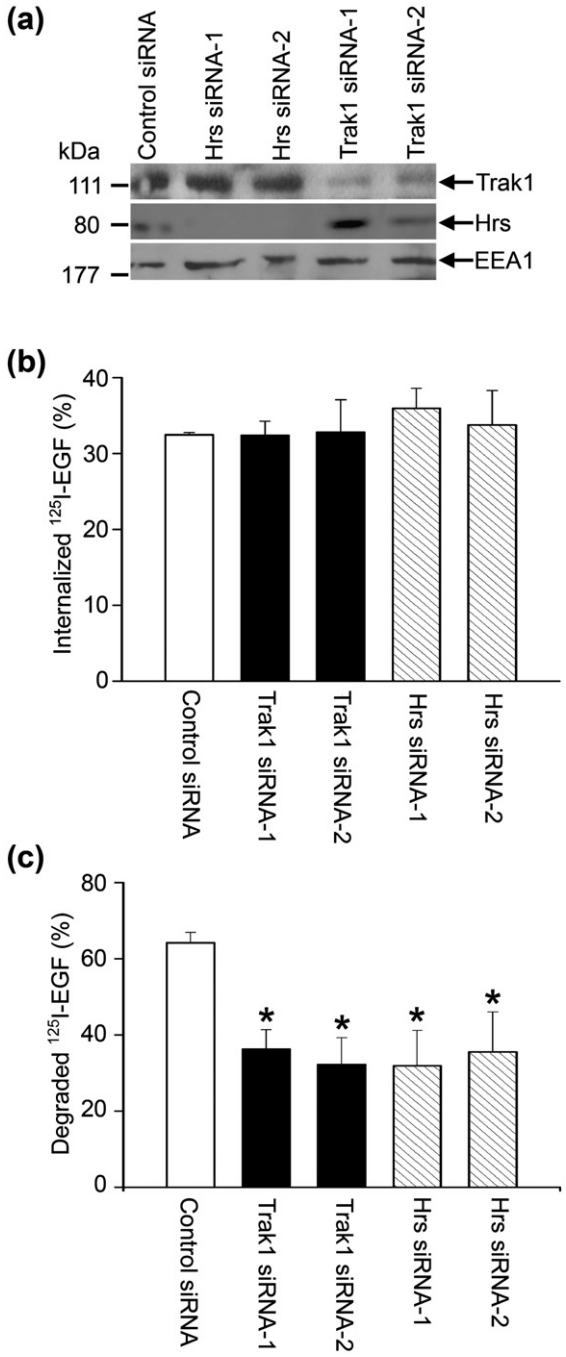

Fig. 8. Trak1 knockdown inhibits degradation, but not endocytosis of [^{125}I]EGF. (a) HeLa cells were transiently transfected with the indicated siRNA constructs. Whole-cell lysates were subjected to SDS-PAGE, followed by immunoblotting with anti-Trak1 or anti-Hrs antibodies. Equal loading was confirmed by immunoblotting with anti-EEA1 antibody. (b) HeLa cells transfected with the indicated siRNAs were incubated with [^{125}I]EGF for 10 min at 37 °C. The internalized [^{125}I]EGF is expressed as a percentage of the initially bound [^{125}I]EGF. (c) HeLa cells transfected with the indicated siRNA constructs were allowed to internalize [^{125}I]EGF for 10 min and then chased for 1 h at 37 °C. The degraded [^{125}I]EGF is expressed as a percentage of the initially internalized [^{125}I]EGF. Data represent the mean ±SEM from three independent experiments. The asterisks indicate a statistically significant difference ($p<0.05$) from the control siRNA-transfected cells.

indicated that overexpression of Trak1 inhibits EGF-induced EGFR degradation by blocking endosome-to-lysosome trafficking of the EGFR. Moreover, Trak1 siRNA experiments showed that Trak1 is required for ligand-induced degradation of the internalized EGF–EGFR complexes, providing further evidence supporting a functional role for Trak1 in the regulation of EGFR endosomal trafficking.

Trak1 is a member of a small family of proteins characterized by the presence of the HAPN domain. Our previous work has shown that the other two members of the HAPN family, HAP1 and GRIF1, both interact with Hrs and regulate endosome-to-lysosome trafficking of internalized EGFRs.[14,15] Thus, the HAPN proteins seem to share a common function as regulators of endosomal trafficking. We and others have shown that these three proteins are differentially expressed; Trak1 is ubiquitously expressed in many tissues and cell types,[7,10] whereas HAP1 and GRIF1 are mainly expressed in the brain, where they are highly enriched in neuronal cells.[7,14,24,25] Moreover, these HAPN proteins may have distinct functions. For example, HAP1 overexpression induces enlarged early endosomes,[15] and GRIF1 overexpression produces perinuclear clustering of endosomes,[14] whereas Trak1 overexpression fails to induce either of these phenotypes. Trak1 and GRIF1 also associate with mitochondria, but HAP1 does not.[11] HAP1 also associates with kinesin light chain,[26] rather than the conventional kinesin heavy chains, which bind to both GRIF1 and Trak1.[9] These similarities and differences among the HAPN proteins suggest that this family of proteins may have overlapping yet distinct functional roles.

In addition to regulating EGFR endosomal trafficking, the HAPN proteins may also regulate trafficking of a variety of cell surface receptors. All three members of the HAPN family have been shown to associate with $GABA_A$ receptor subunits.[10,24,27] In support of this hypothesis, HAP1 has been implicated in the regulation of the endosomal trafficking of $GABA_A$ receptors[27] and the nerve growth factor receptor TrkA.[28] Moreover, the altered levels of $GABA_A$ receptors observed in Trak1 mutant mice[10] suggest that Trak1 may also participate in the regulation of $GABA_A$ receptor endosomal trafficking.

The link between the homozygous Trak1 truncation mutation and a recessively transmitted form of hypertonia[10] suggests that the Trak1 truncation mutation causes hypertonia through a "loss-of-function" mechanism. Based on our finding that Trak1 is a ubiquitously expressed regulator of endosome-to-lysosome trafficking in mammalian cells, one would expect that the Trak1 truncation mutation would lead to dysregulation of endosome-to-lysosome trafficking in many cell types. The hypertonic phenotype of the Trak1 mutant mice suggests that, compared to other cell types, neurons are particularly vulnerable to defects in endosomal trafficking. Consistent with this notion, aberrant endosomal trafficking has recently been implicated in the pathogenesis of a number of neurological diseases. For example, mutations in the endosomal fusion regulators Rab5 guanine nucleotide exchange factor alsin[29] and Vps54[30] cause motor neuron diseases in mammals. Moreover, mutations in the endosomal sorting regulators CHMP2B and Mahogunin cause frontotemporal dementia[31] and spongiform neurodegeneration.[32,33] These lines of genetic evidence provide a direct link between the dysregulation of endosomal trafficking and neuronal dysfunction.

The mechanism by which the Trak1 truncation mutation causes hypertonia is unclear. Our analyses failed to find any difference between Trak1Δhyrt and Trak1 in their localization or function. Previous studies have reported a lack of effect of the Trak1 truncation mutation on the interaction with the $GABA_A$ receptor.[10] Since the kinesin-binding[9] and Hrs-binding[14] domains are outside of the deleted C-terminal region, the Trak1Δhyrt mutation is not expected to affect the ability of Trak1 to bind kinesin or Hrs. In contrast, the Trak1Δhyrt mutation might disrupt the ability of Trak1 to bind the OGT enzyme because truncation of Trak1 at residue 824 deletes a portion of the OGT-binding domain (residues 639–859).[8] Trak1 has been shown to undergo *O*-GlcNAc modification by OGT enzyme,[8] although the functional consequence of this modification has not yet been examined. It is conceivable that the activity of Trak1 may be regulated by posttranslational modifications, such as phosphorylation and *O*-GlcNAc modification,[34,35] and that the Trak1Δhyrt mutation may alter this regulation, thereby leading to neuronal dysfunction. Future studies illuminating the mechanisms of Trak1 action and its regulation should advance our understanding of endosomal trafficking and its dysregulation in hypertonia and other neurological disorders.

Materials and Methods

Antibodies

An anti-Trak1 antibody against the synthetic peptide ILTSGILMGAKLPKQTSLR, corresponding to residues 935–953 of human Trak1, was raised in rabbits. The antibody was affinity-purified as previously described.[36] Other primary antibodies used in this study include the following: anti-Hrs;[36] anti-EEA1 and anti-TIM23 (BD Transduction Laboratories); anti-GFP B2 and anti-GST (Santa Cruz Biotechnologies); anti-KDEL (Stressgen); anti-LAMP2 (H4B4; Developmental Studies Hybridoma Bank, Iowa City, IA); and mouse monoclonal anti-HA (12CA5) antibody. Horseradish-peroxidase-conjugated secondary antibodies and fluorescein-isothiocyanate-, CY5-, or TR-conjugated secondary antibodies (Jackson Immunoresearch Laboratories) were used for immunoblotting and immunostaining, respectively.

Expression constructs

Human full-length Trak1 cDNA (KIAA1042; GenBank accession number AB028965) was a gift from Dr. Takahiro Nagase (Kazusa DNA Institute, Japan). Conventional molecular biological techniques were used to generate

the following expression constructs with N-terminal GFP (pGFP), HA (pHA), or GST (pGST) tags: Trak1 (residues 1–953), Trak1Δhyrt (residues 1–824), Trak1Δ1 (residues 1–419), and Trak1Δ2 (residues 354–953). A schematic representation of the Trak1 constructs is shown in Figs. 4a and 5a. The full-length Hrs expression construct has been described previously.[15,22,36]

Western blot analyses

Cell lysates were homogenized in 1% SDS and subjected to SDS-PAGE. Western blot analysis was carried out as described previously.[14]

In vitro binding assays

His_6-tagged Hrs, GST, or various GST–Trak1 fusion proteins were individually expressed in *Escherichia coli* BL21 cells and purified as described previously.[15,37] *In vitro* binding assays were performed as described previously[15] by incubation of equal amounts of GST or GST–Trak1 fusion proteins immobilized on glutathione agarose beads (Sigma) with soluble His_6-tagged Hrs. Bound proteins were analyzed by SDS-PAGE and immunoblotting.

Cell transfection and immunoprecipitation

HeLa cells were transfected with the indicated plasmids using Lipofectamine 2000 reagent (Invitrogen) in accordance with the manufacturer's instructions. Immunoprecipitations were carried out 24 h posttransfection as described previously[22] using whole-cell lysates and the indicated primary antibodies. Immunocomplexes were then analyzed by SDS-PAGE and immunoblotting.

Immunofluorescence confocal microscopy

HeLa cells were grown on poly-L-lysine-coated glass coverslips. Cells were fixed in 4% paraformaldehyde, stained with appropriate primary and secondary antibodies, and processed for indirect immunofluorescence microscopy as described previously.[15] Analysis and acquisition were performed using a Zeiss LSM 510 confocal laser-scanning microscope. Images were exported in TIFF format using LSM-510 software (Carl Zeiss MicroImaging, Inc.) and processed using Adobe Photoshop CS (Adobe Systems, Inc.).

Quantitative analysis of colocalization

Quantification of the colocalization of Trak1 with various marker proteins (Hrs, EEA1, LAMP2, TIM23, and KDEL) was performed on unprocessed images of cells double-labeled for Trak1 and the indicated marker protein by using Metamorph Imaging System Software (Universal Imaging Corp.) as previously described.[33,38] Briefly, the average gray-scale pixel intensity + 1 SD of a small region of the cell-free area was measured in the Trak1 and marker channels and defined as background. Each field contained several cells, and single cells were manually selected by tracing the cell outlines. Background was subtracted from the cell images by setting the threshold of each channel to the value obtained for the background. The percentage of overlap between Trak1 pixels and Hrs, EEA1, LAMP2, TIM23, or KDEL pixels was determined. For quantification of Trak1 colocalization with each of the marker proteins, 25 cells were randomly selected for analysis. Experiments were repeated at least three times, and the data were subjected to statistical analysis by ANOVA and Tukey's *post hoc* test.

siRNA transfection

Two siRNAs (Dharmacon) were generated against human Trak1 mRNA sequences 3′-UGAAAGAGUU-GGCCAGAUGUU-5′ and 3′-GACGAAGUGUACUGC-CUUAUU-5′, called Trak1 siRNA-1 and siRNA-2, respectively. In addition, a control siRNA with no known mammalian homology (siCONTROL Non-Targeting siRNA no. 1; Dharmacon) was used as negative control. HeLa cells were transfected with the indicated siRNA (100 nM) using the *Trans*IT siQUEST (Mirus) reagent in accordance with the manufacturer's instructions. Forty-eight hours later, the cells were transfected a second time with the siRNA. Experiments were performed 48 h after the final siRNA treatment. For silencing Hrs expression, we used two small hairpin RNAs (shRNAs) targeted against the human Hrs mRNA sequences 3′-CCGGCCGCATGAAGAGTAACCA-CATCTCGAGATGTGGTTACTCTTCATGCGGTTTTTG-5′ and 3′-CCGGGCACGTCTTTCCAGAATTCAACTC-GAGTTGAATTCTGGAAAGACGTGCTTTTTG-5′, called Hrs siRNA-1 and Hrs siRNA-2, respectively (MISSION shRNAs; Sigma). HeLa cells were transfected with the indicated shRNA using Lipofectamine 2000 (Invitrogen) in accordance with the manufacturer's instructions. Experiments were performed 48 h after transfection.

Endocytic trafficking assays

For measurement of TR-transferrin or TR-EGF endocytosis, HeLa cells transfected with the indicated GFP-tagged Trak1 and control plasmids were incubated in serum-free media for 1 h, and then treated with 100 μg/ml TR-transferrin (Invitrogen) at 37 °C for 30 min, or with 3 μg/ml TR-EGF (Invitrogen) in the presence of 0.1% bovine serum albumin (BSA) at 37 °C for 10 min. The cells were then processed for immunofluorescence microscopy.[15] For measurement of TR-EGF trafficking after internalization, cells were washed three times with the media to remove extracellular TR-EGF and incubated for an additional 1, 2, or 3 h at 37 °C prior to fixation and processing for immunofluorescence microscopy.[15] Quantification of the amount of intracellular TR-EGF was performed on unprocessed confocal images of 100 randomly selected transfected cells by using Metamorph Imaging System Software as previously described.[33,38] Background was subtracted from the cell images, and the integrated TR-EGF pixel intensity was determined. Experiments were repeated at least three times, and the data were subjected to statistical analysis by ANOVA and Tukey's *post hoc* test.

[^{125}I]EGF internalization and degradation assays

For measurement of [^{125}I]EGF internalization, HeLa cells transfected with indicated Trak1 and control plasmids were serum-starved for 2 h, then incubated on ice with ~20 ng/ml [^{125}I]EGF (MP Biochemicals) in binding buffer (1% BSA in serum-free DMEM). Cells were then washed with cold binding buffer and either lysed immediately to measure the initially bound [^{125}I]EGF or transferred to 37 °C for 10 min. After the cells had been

washed with acid wash (0.5 M NaCl and 0.2 M acetic acid, pH 2.8) on ice, the internalized [^{125}I]EGF was measured as described[39,40] and expressed as a percentage of the initially bound [^{125}I]EGF. For measurement of [^{125}I]EGF degradation after internalization, transfected HeLa cells were incubated with [^{125}I]EGF at 37 °C for 10 min and then acid-washed to remove unbound and surface-bound [^{125}I]EGF. Cells were then lysed to measure the internalized [^{125}I]EGF or chased in serum-free DMEM containing 1.5 μg/ml EGF and 1% BSA at 37 °C for 1, 2, or 3 h. The amount of [^{125}I]EGF remaining in the cells at the indicated chase time point was measured as described.[39,40] The amount of degraded [^{125}I]EGF was determined by subtraction of the remaining [^{125}I]EGF from the internalized [^{125}I]EGF and was expressed as a percentage of the internalized [^{125}I]EGF. All measurements of [^{125}I]EGF levels were performed by determining radioactivity (^{125}I counts per minute) in a Wallac Wizard 1470 Automatic Gamma Counter. Data were obtained from at least three independent experiments and analyzed by ANOVA and Tukey's *post hoc* test.

Acknowledgements

We thank Dr. Takahiro Nagase (Kazusa DNA Research Institute, Japan) for the gift of KIAA1042 cDNA, and Sharon Swanger (Emory University) for assistance in generating the Trak1 deletion constructs. This work was supported by grants from the National Institutes of Health (NS050650, NS047575, and ES015813).

References

1. Katzmann, D. J., Odorizzi, G. & Emr, S. D. (2002). Receptor downregulation and multivesicular-body sorting. *Nat. Rev. Mol. Cell Biol.* **3**, 893–905.
2. Waterman, H. & Yarden, Y. (2001). Molecular mechanisms underlying endocytosis and sorting of ErbB receptor tyrosine kinases. *FEBS Lett.* **490**, 142–152.
3. Mullins, C. & Bonifacino, J. S. (2001). The molecular machinery for lysosome biogenesis. *BioEssays*, **23**, 333–343.
4. Yan, Q., Sun, W., Kujala, P., Lotfi, Y., Vida, T. A. & Bean, A. J. (2005). CART: an Hrs/actinin-4/BERP/myosin V protein complex required for efficient receptor recycling. *Mol. Biol. Cell*, **16**, 2470–2482.
5. Hanyaloglu, A. C., McCullagh, E. & von Zastrow, M. (2005). Essential role of Hrs in a recycling mechanism mediating functional resensitization of cell signaling. *EMBO J.* **24**, 2265–2283.
6. Nickerson, D. P., Russell, M. R. & Odorizzi, G. (2007). A concentric circle model of multivesicular body cargo sorting. *EMBO Rep.* **8**, 644–650.
7. Iyer, S. P., Akimoto, Y. & Hart, G. W. (2003). Identification and cloning of a novel family of coiled-coil domain proteins that interact with *O*-GlcNAc transferase. *J. Biol. Chem.* **278**, 5399–5409.
8. Iyer, S. P. & Hart, G. W. (2003). Roles of the tetratricopeptide repeat domain in *O*-GlcNAc transferase targeting and protein substrate specificity. *J. Biol. Chem.* **278**, 24608–24616.
9. Brickley, K., Smith, M. J., Beck, M. & Stephenson, F. A. (2005). GRIF-1 and OIP106, members of a novel gene family of coiled-coil domain proteins: association *in vivo* and *in vitro* with kinesin. *J. Biol. Chem.* **280**, 14723–14732.
10. Gilbert, S. L., Zhang, L., Forster, M. L., Iwase, T., Soliven, B., Donahue, L. R. *et al.* (2006). Trak1 mutation disrupts GABA(A) receptor homeostasis in hypertonic mice. *Nat. Genet.* **38**, 245–250.
11. Fransson, S., Ruusala, A. & Aspenstrom, P. (2006). The atypical Rho GTPases Miro-1 and Miro-2 have essential roles in mitochondrial trafficking. *Biochem. Biophys. Res. Commun.* **344**, 500–510.
12. Lupas, A., Van Dyke, M. & Stock, J. (1991). Predicting coiled coils from protein sequences. *Science*, **252**, 1162–1164.
13. Berger, B., Wilson, D. B., Wolf, E., Tonchev, T., Milla, M. & Kim, P. S. (1995). Predicting coiled coils by use of pairwise residue correlations. *Proc. Natl Acad. Sci. USA*, **92**, 8259–8263.
14. Kirk, E., Chin, L. S. & Li, L. (2006). GRIF1 binds Hrs and is a new regulator of endosomal trafficking. *J. Cell Sci.* **119**, 4689–4701.
15. Li, Y., Chin, L. S., Levey, A. I. & Li, L. (2002). Huntingtin-associated protein 1 interacts with hepatocyte growth factor-regulated tyrosine kinase substrate and functions in endosomal trafficking. *J. Biol. Chem.* **277**, 28212–28221.
16. Mizushima, N. (2007). Autophagy: process and function. *Genes Dev.* **21**, 2861–2873.
17. Olzmann, J. A., Li, L., Chudaev, M. V., Chen, J., Perez, F. A., Palmiter, R. D. & Chin, L. S. (2007). Parkin-mediated K63-linked polyubiquitination targets misfolded DJ-1 to aggresomes via binding to HDAC6. *J. Cell Biol.* **178**, 1025–1038.
18. Glater, E. E., Megeath, L. J., Stowers, R. S. & Schwarz, T. L. (2006). Axonal transport of mitochondria requires Milton to recruit kinesin heavy chain and is light chain independent. *J. Cell Biol.* **173**, 545–557.
19. Morino, C., Kato, M., Yamamoto, A., Mizuno, E., Hayakawa, A., Komada, M. & Kitamura, N. (2004). A role for Hrs in endosomal sorting of ligand-stimulated and unstimulated epidermal growth factor receptor. *Exp. Cell Res.* **297**, 380–391.
20. Mellman, I. (1996). Endocytosis and molecular sorting. *Annu. Rev. Cell Dev. Biol.* **12**, 575–625.
21. Mellman, I. (1996). Membranes and sorting. *Curr. Opin. Cell Biol.* **8**, 497–498.
22. Chin, L. S., Raynor, M. C., Wei, X., Chen, H. Q. & Li, L. (2001). Hrs interacts with sorting nexin 1 and regulates degradation of epidermal growth factor receptor. *J. Biol. Chem.* **276**, 7069–7078.
23. Kanazawa, C., Morita, E., Yamada, M., Ishii, N., Miura, S., Asao, H. *et al.* (2003). Effects of deficiencies of STAMs and Hrs, mammalian class E Vps proteins, on receptor downregulation. *Biochem. Biophys. Res. Commun.* **309**, 848–856.
24. Beck, M., Brickley, K., Wilkinson, H. L., Sharma, S., Smith, M., Chazot, P. L. *et al.* (2002). Identification, molecular cloning, and characterization of a novel $GABA_A$ receptor-associated protein, GRIF-1. *J. Biol. Chem.* **277**, 30079–30090.
25. Li, X. J., Li, S. H., Sharp, A. H., Nucifora, F. C., Jr., Schilling, G., Lanahan, A. *et al.* (1995). A huntingtin-associated protein enriched in brain with implications for pathology. *Nature*, **378**, 398–402.
26. McGuire, J. R., Rong, J., Li, S. H. & Li, X. J. (2006). Interaction of Huntingtin-associated protein-1 with kinesin light chain: implications in intracellular trafficking in neurons. *J. Biol. Chem.* **281**, 3552–3559.

27. Kittler, J. T., Thomas, P., Tretter, V., Bogdanov, Y. D., Haucke, V., Smart, T. G. & Moss, S. J. (2004). Huntingtin-associated protein 1 regulates inhibitory synaptic transmission by modulating {gamma}-aminobutyric acid type A receptor membrane trafficking. *Proc. Natl Acad. Sci. USA*, **101**, 12736–12741.
28. Rong, J., McGuire, J. R., Fang, Z. H., Sheng, G., Shin, J. Y., Li, S. H. & Li, X. J. (2006). Regulation of intracellular trafficking of huntingtin-associated protein-1 is critical for TrkA protein levels and neurite outgrowth. *J. Neurosci.* **26**, 6019–6030.
29. Yang, Y., Hentati, A., Deng, H. X., Dabbagh, O., Sasaki, T., Hirano, M. *et al.* (2001). The gene encoding alsin, a protein with three guanine-nucleotide exchange factor domains, is mutated in a form of recessive amyotrophic lateral sclerosis. *Nat. Genet.* **29**, 160–165.
30. Schmitt-John, T., Drepper, C., Mussmann, A., Hahn, P., Kuhlmann, M., Thiel, C. *et al.* (2005). Mutation of Vps54 causes motor neuron disease and defective spermiogenesis in the wobbler mouse. *Nat. Genet.* **37**, 1213–1215.
31. Skibinski, G., Parkinson, N. J., Brown, J. M., Chakrabarti, L., Lloyd, S. L., Hummerich, H. *et al.* (2005). Mutations in the endosomal ESCRTIII-complex subunit CHMP2B in frontotemporal dementia. *Nat. Genet.* **37**, 806–808.
32. He, L., Lu, X. Y., Jolly, A. F., Eldridge, A. G., Watson, S. J., Jackson, P. K. *et al.* (2003). Spongiform degeneration in mahoganoid mutant mice. *Science*, **299**, 710–722.
33. Kim, B. Y., Olzmann, J. A., Barsh, G. S., Chin, L. S. & Li, L. (2007). Spongiform neurodegeneration-associated E3 ligase Mahogunin ubiquitilates TSG101 and regulates endosomal trafficking. *Mol. Biol. Cell*, **18**, 1129–1142.
34. Zachara, N. E. & Hart, G. W. (2006). Cell signaling, the essential role of *O*-GlcNAc! *Biochim. Biophys. Acta*, **1761**, 599–617.
35. Zachara, N. E. & Hart, G. W. (2004). *O*-GlcNAc a sensor of cellular state: the role of nucleocytoplasmic glycosylation in modulating cellular function in response to nutrition and stress. *Biochim. Biophys. Acta*, **1673**, 13–28.
36. Kwong, J., Roundabush, F. L., Hutton Moore, P., Montague, M., Oldham, W., Li, Y. *et al.* (2000). Hrs interacts with SNAP-25 and regulates Ca(2$^+$)-dependent exocytosis. *J. Cell Sci.* **113**, 2273–2284.
37. Chin, L. S., Nugent, R. D., Raynor, M. C., Vavalle, J. P. & Li, L. (2000). SNIP, a novel SNAP-25-interacting protein implicated in regulated exocytosis. *J. Biol. Chem.* **275**, 1191–1200.
38. Volpicelli, L. A., Lah, J. J. & Levey, A. I. (2001). Rab5-dependent trafficking of the m4 muscarinic acetylcholine receptor to the plasma membrane, early endosomes, and multivesicular bodies. *J. Biol. Chem.* **276**, 47590–47598.
39. Valiathan, R. R. & Resh, M. D. (2004). Expression of human immunodeficiency virus type 1 gag modulates ligand-induced downregulation of EGF receptor. *J. Virol.* **78**, 12386–12394.
40. Longva, K. E., Blystad, F. D., Stang, E., Larsen, A. M., Johannessen, L. E. & Madshus, I. H. (2002). Ubiquitination and proteasomal activity is required for transport of the EGF receptor to inner membranes of multivesicular bodies. *J. Cell Biol.* **156**, 843–854.